Chemistry–A European Journal
Research Article
doi.org/10.1002/chem.202304007
Chemistry Europe
European Chemical Societies Publishing
www.chemeurj.org

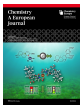

Enantioselective Total Synthesis of the Morphogen (−)-Thallusin and Mediated Uptake of Fe(III) into the Green Seaweed *Ulva*

Paul Wienecke,[a] Johann F. Ulrich,[b] Cristina F. Morales-Reyes,[b, d] Seema Dhiman,[a, c] Thomas Wichard,*[b] and Hans-Dieter Arndt*[a]

A fully enantioselective, catalytic synthesis of the algal morphogen (−)-thallusin using polyene cyclization chemistry is reported. The synthesis features dedicated precursor design, introduction of a TMS-substituted arene as a regioselective terminator, very high enantiomer excess (*ee*) on gram scale, and productive scaffold functionalization. Furthermore, an *ee* determination methodology of thallusin samples was developed, and the *ee* of biosynthesized thallusin was determined. Fe(III)-uptake studies demonstrated that the cellular uptake of iron facilitated by thallusin derivatives was independent of their morphogenic activity, suggesting their active import via siderophore transporters as a shuttle system.

Introduction

The industrial cultivation of marine algae is highly promising for the production of fuel, food and fine chemicals directly from atmospheric CO_2.[1] Marine algae typically convert solar energy far more efficiently to biomass than terrestrial plants do.[2] Furthermore, cultivation may be pursued on land unsuitable for farming or even in wastewater treatment.[3] For production processes from algal biomass, defined cultivation conditions ensuring constant quality and sustainability are key.[4] Therefore, understanding the algal growth process and the factors involved is highly important for controlled algal aquacultures.[5] Such insight will also contribute to elucidating the emergence of algal blooms, a phenomenon with tremendous socioeconomic impact.[6]

(−)-Thallusin (**1**, Scheme 1), a terpenoid natural product, possesses distinct functions in algal development, with differences depending on the recipient.[7,8] Thallusin was originally found to promote stable thallus formation in *Gayralia oxyspermum*.[9] However, in the cosmopolitan green marine macroalgae *Ulva compressa* (cultivar *mutabilis*), (−)-**1** induces rhizoid formation and cell wall development.[7] Without this algal growth and morphogenesis-promoting factor (AGMPF), cell walls are covered with protrusions and no rhizoid is formed.[10] Both its high activity and the distinct responses of different organisms make stereo-selective syntheses of thallusin and its derivatives necessary for understanding the uptake and signal transduction of this morphogenetic compound.

Thallusin is only secreted by a few symbiotic bacteria, such as *Maribacter* spp. and *Zobellia* spp.[7,9,11] Combined with *Roseovarius* sp. MS2, which provides a further unknown AGMPF, a tripartite community of *Ulva-Roseovarius-Maribacter* is formed that completes the induction of morphogenesis in *Ulva*.[10–12] Interestingly, the algae have been shown to import Fe(III) specifically by a 2:1 thallusin-Fe(III)-complex (**1a**), presumably formed by the dipicolinic acid moiety as a chelating unit.[7] To date, the molecular mode of action of thallusin and the role of its corresponding Fe(III)-complex remain to be defined.

The amounts of thallusin required for in-depth studies and application cannot be obtained efficiently by fermentation (yield $< 1\ \mu g \cdot L^{-1}$). In the first published synthesis, (+)-*ent*-thallusin was obtained from sclareol oxide, clarifying the stereochemistry of **1**.[13] *Ent*-thallusin was shown to be biologically inactive in *M. oxyspermum*. A follow-up study revealed no influence of a racemic mixture on the morphogenic activity of the natural enantiomer.[14] This was confirmed by a second racemic synthesis using a Hg^{2+}-promoted polycyclization.[15] Enantiopure (−)-thallusin was finally obtained by enzymatic resolution of a racemic intermediate.[16] Recently, we have

[a] P. Wienecke, S. Dhiman, H.-D. Arndt
Friedrich Schiller University Jena
Institute of Organic Chemistry and Macromolecular Chemistry
Humboldtstr. 10
D-07743 Jena (Germany)
E-mail: hd.arndt@uni-jena.de

[b] J. F. Ulrich, C. F. Morales-Reyes, T. Wichard
Friedrich Schiller University Jena
Institute of Inorganic and Analytical Chemistry
Lessingstr. 8
D-07743 Jena (Germany)
E-mail: thomas.wichard@uni-jena.de

[c] S. Dhiman
New address: SRM University
Department of Chemistry
Andhra Pradesh 522502 (India)

[d] C. F. Morales-Reyes
New address: Universidad de Santiago de Chile (USACH)
Facultad de Química y Biología
Santiago 9170022 (Chile)

Supporting information for this article is available on the WWW under https://doi.org/10.1002/chem.202304007

reported a fully stereoselective total synthesis of (−)-thallusin using a resolution strategy with a chiral-auxiliary.[17] Thereby an extraordinarily potent and stereoselective morphogenic activity was found in *Ulva* (EC_{50} = 4.9 pmol L^{-1}). Noteworthy, structure-activity-relationship (SAR) analysis indicated a pathway-selective activity triggered by certain structural elements.[17]

To gain potentially scalable access to its terpene framework, we were interested in developing an improved, catalytic and enantioselective total synthesis of (−)-thallusin by using an asymmetric polyene cyclization. In contrast to resolution, material throughput should be more effective, and greater flexibility regarding derivatizations might be realized. Furthermore, we aimed to study the origin of the extraordinarily high bioactivity, the differentiation of stereoisomers, and the role of the Fe(III)-complex in thallusin function.

Synthesis Planning. We envisioned (−)-thallusin (**1**) to be synthesized by using a sp^2-sp^2-coupling of enol (pseudo−)halide **2** with a pyridine fragment (Scheme 2A). Compound **2**, bearing a suitable carboxylic acid surrogate group R at the dihydropyran moiety, was planned to arise from lactone **3**, the enantiomer of the natural product (+)-ambreinolide. We recently reported an efficient multigram-scale synthesis of racemic ambreinolide by using a proton-initiated polyene cyclization of anisole **4** as the key step.[18] This Lewis-acid assisted, chiral Brønsted-acid based method however provided only modest enantioselectivity. For improved efficiency, we aimed to access enantiopure lactone **3** by an alternative approach. The success of polyene cyclizations depends on the right combination of the initiating functional group, the activator, and the terminating unit, to ensure the selective formation of a single product.[19] Many reported methods demand a nucleophilic alcohol as an efficient terminator,[20] but we found this feature difficult to implement. Instead, we envisioned an aromatic terminator that should conclude a cationic cascade by rearomatization, thereby providing one product selectively. An anisole moiety was expected to be sufficiently nucleophilic and could serve as a template for further functionalization. The enantioselectivity of polyene cyclization mainly relies on the choice of initial leaving group and (chiral) activator. After the first asymmetric ring closure, the subsequent cyclizations follow the Stork–Eschenmoser postulate, i.e. *trans*-alkenes form *trans* ring-junctions, and *cis*-alkenes form *cis* ring-junctions.[21–23] A potentially suitable initiator might be an allylic alcohol as a precursor of a chiral cationic iridium complex for initiating a polyene cyclization with high enantioselectivity.[24] The resulting product may be easily transformed into the desired dimethyl group of lactone **3**. The

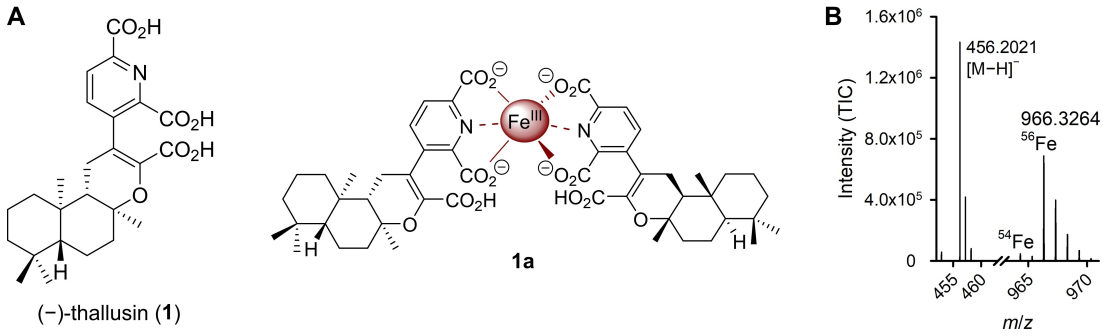

Scheme 1. (**A**) Structure of (−)-thallusin (**1**) and proposed structure of 2 : 1 thallusin-Fe(III) complex (**1 a**). (**B**) Electrospray ionization mass spectrometry of $[Fe^{III}(2Thal\text{-}4H)]^-$, measured in negative ionization mode. Isotopologues containing ^{54}Fe or ^{56}Fe are indicated.

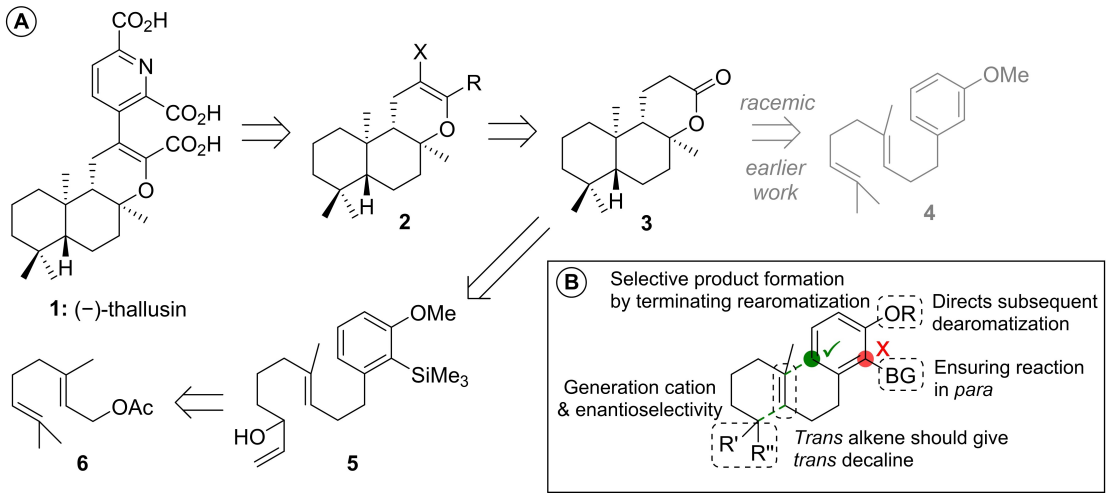

Scheme 2. (A) Retrosynthetic analysis of (−)-thallusin (**1**); (B) Design rationale for the polyene cyclization substrate (BG = blocking group).

design rationale for the polyene cyclization substrate is summarized in Scheme 2B.

Unfortunately, the literature[24] and preliminary studies had indicated that monosubstituted aromatic terminators will produce two regioisomers unselectively. A suitable blocking group on the anisole ortho-position was envisioned to ensure regioselectivity. Among different substituents, a trimethylsilyl group seemed promising due to its simple, traceless removal. So far, this moiety has only been applied to blocking aromatic positions against lithiation.[25–27] During reactions with electrophilic reagents, arylsilane groups typically electronically activate the *ipso*-position.[28–30] This canonical reactivity could promote undesired regioselectivity, but steric hindrance was envisioned to disfavor this undesired pathway, and to guide ring closure in the intended mode (Scheme 3). Electronic activation by the β-Si effect would still enhance reactivity in *meta*-position of the silyl substituent.[31]

Lactone **3** would be obtained by dearomatization and skeletal refunctionalization of the polyene cyclization product. Precursor **5** was planned to arise from commercial geranyl acetate (**6**). Establishing a synthesis route from lactone **3** to thallusin (**1**) should also allow facile preparation of racemic thallusin by using a racemic polyene cyclization.[18] Furthermore, enol triflate **2** could serve as an attractive starting point for SAR studies due to the versatility of carboxylic acid surrogates and the possibility of introducing different aromatic moieties at the coupling site.

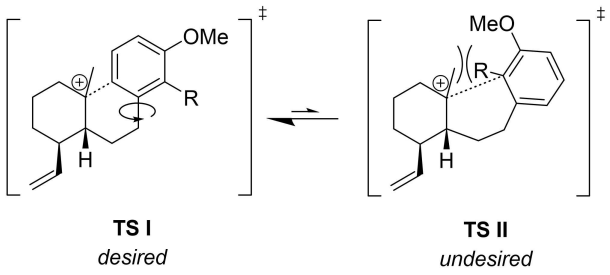

Scheme 3. Anticipated transition state (TS) arrangements I and II during the second ring closure of the polyene cyclization (R = TMS). Although a quasi-concerted mechanism for this transformation is likely, a stepwise depiction was selected for illustration purposes.

Results and Discussion

Enantioselective polyene cyclization. The synthesis of the polyene cyclization precursor **5** commenced with regioselective epoxidation of geranyl acetate's (**6**) terminal double bond, followed by periodate cleavage of the diol formed *in situ* (Scheme 4). The resulting aldehyde was then reduced to the alcohol, mesylated, and transformed to nitrile **7** by substitution with cyanide, with a 62% yield over five steps on decagram-scale. To provide the 1,2,3-trisubstituted arene, benzylic alcohol **9** was subjected to alkoxide-directed *ortho*-lithiation[32] and trapped with TMSCl. The intermediate silyl ether was cleaved, and benzylic chlorination gave compound **10** in a very good overall yield (64%). Benzyl chloride **10** was coupled to the allylic acetate **7** by using a S_N2-selective substitution with a cuprate derived from its corresponding Grignard reagent.[33] The resulting nitrile **8** was transformed into allylic alcohol **5** by DIBAL–H reduction to the aldehyde, followed by addition of vinyl Grignard reagent (67% yield).

To our delight, applying Carreira's iridium catalyst, generated *in situ* from ligand **11**,[24] produced decaline **12** as polyene cyclization product in very good yield (89%) and excellent enantioselectivity (>98% *ee*, Scheme 5), even on multigram-scale (>97% *ee*). As intended, the TMS group rendered the second ring closure fully regioselective, validating our blocking concept, and was easily removed by treatment with acid. To introduce the *gem*-dimethyl group at the decalin core, the vinyl group was degraded by Lemieux-Johnson oxidation. The resulting aldehyde was α-methylated and reduced (Scheme 5).

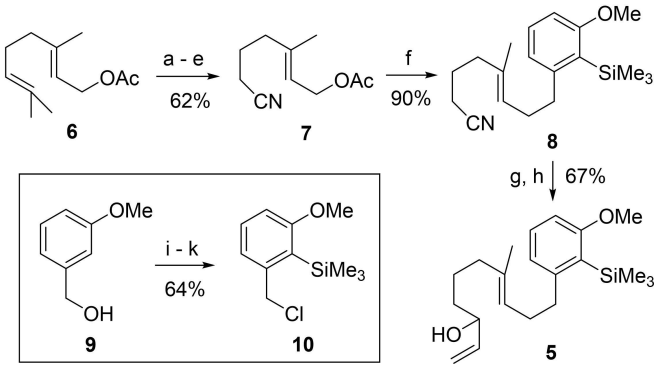

Scheme 4. Synthesis of polyene cyclization substrate **5**. Reagents and conditions: a) *m*CPBA (1.0 equiv), CH_2Cl_2, −10 °C to r.t.; b) H_5IO_6 (1.0 equiv), THF/Et_2O, 0 °C; c) $NaBH_4$ (1.1 equiv), THF/H_2O; d) MsCl (1.5 equiv), Et_3N (3.0 equiv), CH_2Cl_2, 0 °C to r.t.; e) NaCN (3.0 equiv), DMF, 50 °C, 62% from **6**; f) **10** (1.5 equiv), Mg^0 (18.0 equiv), Li_2CuCl_4 (15 mol%), THF/Et_2O, 0 °C, 90%; g) DIBALH (1.2 equiv), toluene/CH_2Cl_2, -78 °C; h) VinylMgCl (1.1 equiv), THF, −78 °C to 0 °C, 67% from **8**; i) i. *n*BuLi (2.1 equiv), toluene/hexane, -40 °C to r.t., ii. TMSCl (2.1 equiv), THF, −78 °C to r.t.; j) 1 M HCl (1.0 equiv), MeOH, 0 °C, 71% from **9**; k) MsCl (4.0 equiv), Et_3N (2.0 equiv), CH_2Cl_2, 0 °C to r.t., 90%.

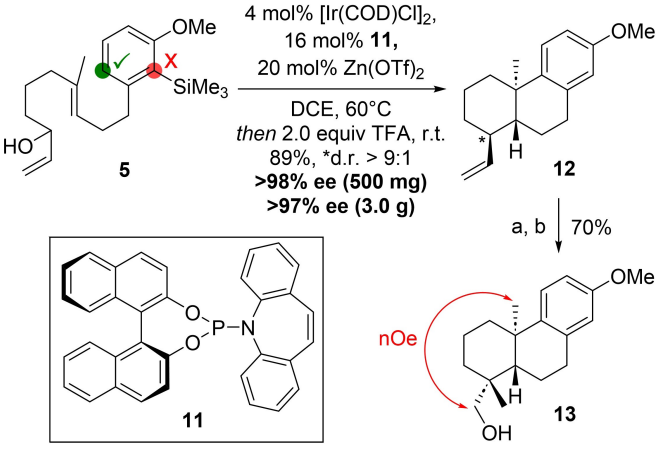

Scheme 5. Enantioselective polyene cyclization of allylic alcohol **5** and vinyl group transformation to alcohol **13**. Reagents and conditions: a) OsO_4 (5 mol%), NMO (3.0 equiv), H_2O, THF, *t*BuOH, r.t. *then* $NaIO_4$ (3.0 Äqu), r.t., 81%; b) KO*t*Bu (10.0 equiv), MeI (10.0 equiv), *t*BuOH, 0 °C to r.t. *then* $NaBH_4$ (7.0 equiv), H_2O, r.t., 87%.

The resulting alcohol **13** was obtained as a single diastereomer (NOE), presumably because of the α-face alkylation of the intermediate aldehyde enolate.[34]

Synthesis of *ent*-ambreinolide. The anisole moiety of compound **13** was reductively dearomatized by Birch reduction, and acidic hydrolysis of the resulting enol ether gave enone **14** diastereoselectively (Scheme 6). Treatment of enone **14** with *m*CPBA resulted in Baeyer-Villiger oxidation and further epoxidation of the intermediate enol. PCC oxidation of the primary alcohol yielded aldehyde **15**, setting the stage for double deoxygenation.[26] Base-induced epoxy lactone rearrangement in the presence of hydrazine hydrate gave dihydrazone **16**. On heating, this compound underwent double Wolff-Kishner reduction to give carboxylic acid **17**.[35,36] Finally, cationic lactonization of carboxylic acid **17** by using sulfuric acid provided *ent*-ambreinolide (**3**).

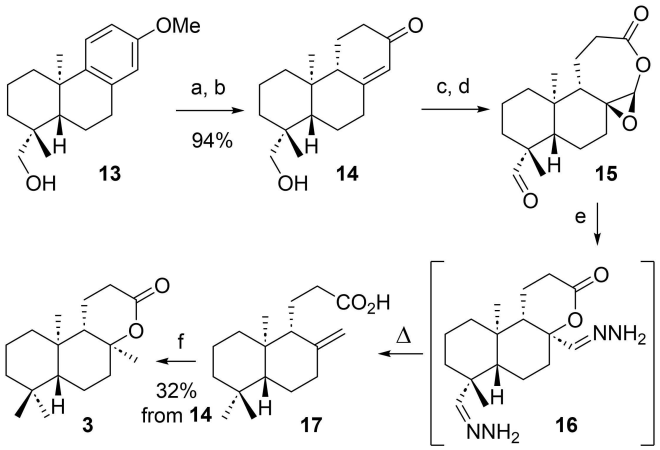

Scheme 6. Synthesis of lactone **3** from alcohol **13**. Reagents and conditions: a) Li^0 (6.5 equiv), NH_3 (l), THF, −78 °C, *then* EtOH, −40 °C; b) 1 M HCl, MeOH, reflux, 94% from **13**; c) *m*CPBA (4.0 equiv), CH_2Cl_2, r.t.; d) PCC (4.0 equiv), CH_2Cl_2, r.t.; e) KOH (23 equiv), $H_2NNH_2{\cdot}H_2O$, diethylene glycol, r.t. *then* 120 °C to 210 °C; f) H_2SO_4, AcOH, −10 °C, 32% from **14**.

Scaffold functionalization chemistry. With a synthetic route to enantiopure lactone **3** in hand, we explored the assembly of the unique dihydropyrane-pyridine framework of thallusin bearing three carboxyl groups. Initially, lactone **3** was converted to carboxylic ester **18** by a palladium-catalyzed CO-free carbonylation of the corresponding enol triflate (Scheme 7, path A).[37] Carboxylic ester **18** was iodinated[38] and transesterified to vinyl iodide **19** as the first targeted coupling substrate to introduce the pyridine fragment. Despite extensive screening of the reaction conditions, no sp^2-sp^2 cross-coupling or borylation for subsequent Suzuki-Miyaura coupling to the sought pyridine **20** could be achieved, indicating electronic deactivation and unfavorable strain imposed by the highly substituted vinyl halide substrate.

To possibly reduce strain, lactone **3** was reduced to the corresponding lactol, which yielded dihydropyran **21** after elimination (Scheme 7, path B). An attempt of enol ether α-cyanation by halogenation, substitution with cyanide, and elimination, failed.[39,40] However, direct electrophilic cyanation

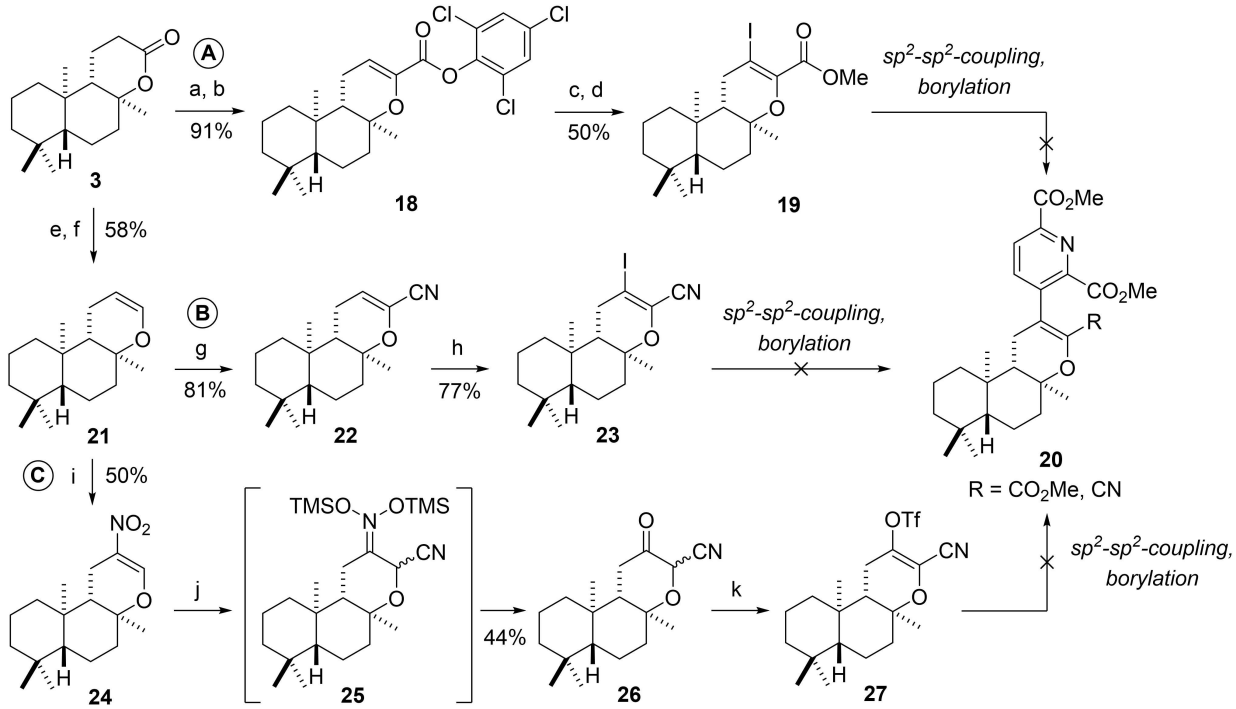

Scheme 7. Synthetic attempts from lactone **3** to pyridine **20**. Reagents and conditions: a) KHMDS (2.4 equiv), $PhNTf_2$ (1.9 equiv), THF, toluene, −78 °C; b) $Pd(OAc)_2$ (6 mol%), XantPhos (12 mol%), 2,4,6-trichlorophenyl formate (1.4 equiv), Et_3N (1.4 equiv), r.t., 91% from **3**; c) NIS (1.2 equiv), $AgNO_3$ (0.2 equiv), MeCN, 70 °C, 62%; d) K_3PO_4 (3.0 equiv), MeOH (2.5 equiv), DMF, 80%; e) DIBALH (1.1 equiv), toluene, −78 °C; f) MsCl (2.5 equiv), Et_3N (8.0 equiv), THF, 0 °C to r.t., 58% from **3**; g) NIS (1.2 equiv), TMSCN (9.0 equiv), $Zn(OTf)_2$ (0.1 equiv), CH_2Cl_2, r.t. *then* DBU (2.0 equiv), r.t., 81%; h) NIS (2.8 equiv), $AgNO_3$ (0.3 equiv), MeCN, 70 °C, 77%; i) HNO_3 (5.0 equiv), Ac_2O, 0 °C to −30 °C, 50%; j) acetone cyanohydrin (4.0 equiv), KCN (0.1 equiv), 18-crown-6 (0.1 equiv), r.t. *then* DBU (1.5 equiv), TMSCl (2.3 equiv), 0 °C *then* *m*CPBA (1.7 equiv), 0 °C to r.t., 44%, d.r. >4:1); k) KHMDS (1.2 equiv), $PhNTf_2$ (1.1 equiv), THF, −78 °C.

to nitrile **22** using ICN generated *in situ*[41] was successful (81% yield), and iodination provided the substrate **23**. Unfortunately, sp^2-sp^2-coupling and borylation attempts remained unsuccessful again for iodide **23**. Likewise, metal-halogen exchange by organolithium bases or "turbo-Grignard"[42] was unproductive.

Previous studies have suggested that enol triflates can be advantageous in cross-coupling reactions compared to vinyl halides in conjugated substrates.[43] Therefore, we pursued the synthesis of α-cyano-β-trifluoromethanesulfonate dihydropyran **27**. For the required glycoside-like α-cyano-β-keto motif in precursor **26**, no synthetic access has been reported so far. A related preparation attempt from a glycosyl bromide failed.[44] Our successful transformation commenced with the nitration of dihydropyran **21**, using *in situ*–generated acetyl nitrate, giving nitro compound **24** (50%, Scheme 7, path C). Utilizing the nitroalkene Michael acceptor properties,[45] we screened for cyanation conditions to introduce the nitrile group. Although the tendency of nitroalkene **24** for polymerization was troubling, an effective 1,4-addition of cyanide was achieved in an aprotic solvent by using acetone cyanohydrine as a cyanide donor.[46] The resulting nitronate was silylated to silyl nitronate **25** and treated with *m*CPBA, effecting a Nef-like oxidation,[47] to provide the desired α-cyano tetrahydropyran-2-one **26** in a one-pot fashion. Accessing this unprecedented structural motif may benefit diverse carbohydrate and natural product synthesis. However, as before, cross-coupling and borylation attempts of the easily prepared triflate **27** remained unproductive in our case.

Completion of (−)-thallusin total synthesis. The cross-conjugated double bond seemed to be particularly deactivated towards sp^2-sp^2 couplings. Therefore, we investigated a substrate bearing a non-conjugated double bond. To this end lactone **3** was sequentially oxidized by using Davis reagent[48] and Dess Martin periodinane, to provide α-keto lactone **28** (68% yield, Scheme 8). Triflation, DIBAL–H reduction, trapping of the resulting lactol with acetic anhydride, and $Zn(OTf)_2$-catalyzed substitution of the acetoxy group by TMSCN then produced the nitrile **2** in good yield. By employing organozinc reagent **29**, the pyridine fragment of thallusin was efficiently connected to the non-conjugated enol triflate **2** by a Negishi coupling, strongly indicating that the conjugated enol electrophiles (**19**, **23**, **27**) were electronically deactivated and/or sterically too demanding. Basic hydrolysis of the carboxylate and nitrile groups of compound **30** then isomerized the olefin into conjugation, cleanly leading to (−)-thallusin (**1**). To gain further insights into the biological relevance of the carboxylic acid on the terpenoid framework, we also prepared the nitrile analogue **31** by anhydrous double-bond isomerization of compound **30** and selective saponification of its ester moieties (80%).

Determination of enantiomeric excess. Considering the astonishing potency of thallusin, even traces of contamination of the active isomer might skew the interpretation of biological activity tests. However, *ee* determinations of polar compounds that form metal ion complexes may be problematic. To develop a reliable HPLC-based method for *ee* determination of thallusin samples, we adapted our derivatization-based workflow for thallusin analytics.[49] A first *ee* determination was undertaken with (−)-thallusin samples taken from the synthesis described before. After derivatization with iodomethane, the thallusin methyl ester enantiomers were separated on a chiral amylose column with a proper resolution factor ($R = 2.6$, Figure 1). The measured *ee* of 97.7% was in excellent agreement with our intermediate *ee* determination during synthesis. Chiral separation of (−)-**1** ($t_R = 21.2$ min) revealed only traces of the biologically inactive isomer (+)-**1** ($t_R = 19.1$ min). Importantly,

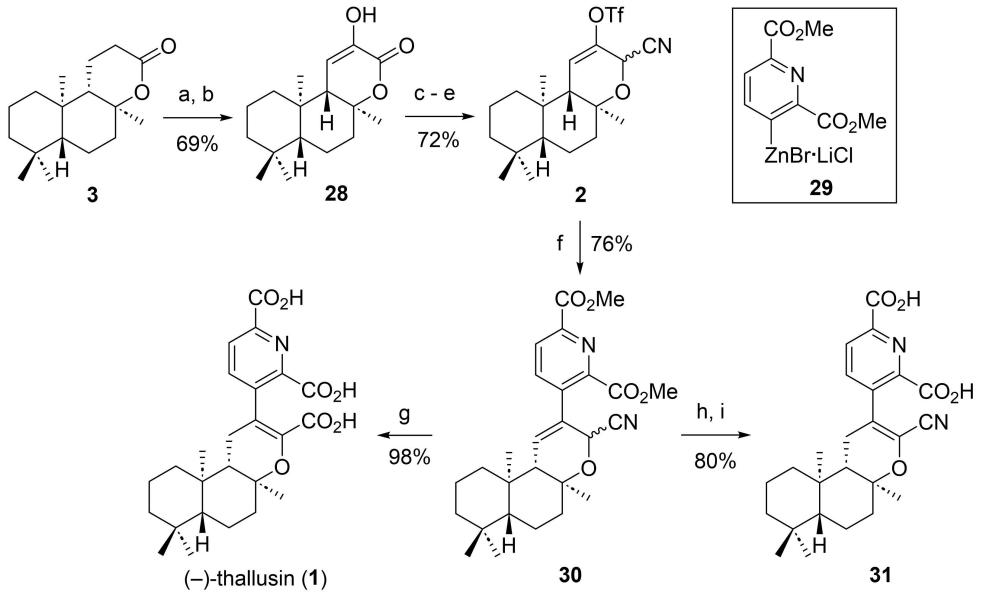

Scheme 8. Synthesis of thallusin (**1**) and derivative **31**. a) KHMDS (2.0 equiv), (1*R*)-(−)-(10-camphorsulfonyl)oxaziridine (2.0 equiv), THF, toluene, −78 °C, 71%; b) DMP (2.0 equiv), CH_2Cl_2, r.t., 97%; c) Tf_2O (3.0 equiv), Et_3N (3.0 equiv), CH_2Cl_2, 0 °C; d) DIBALH (1.2 equiv), CH_2Cl_2, −78 °C *then* pyridine (5.0 equiv), DMAP (3.0 equiv), Ac_2O (5.0 equiv), −78 °C to 0 °C; e) TMSCN (4.2 equiv), $Zn(OTf)_2$ (6 mol%), MeCN, r.t., 72% from **28**, d.r. = 3 : 2); f) **29** (3.0 equiv), $Pd(PPh_3)_4$ (5 mol%), THF, r.t., 76%; g) NaOH (25 equiv), EtOH, H_2O, 100 °C, 98%; h) DBU (1.0 equiv), toluene, 80 °C, 80%; i) $LiOH{\cdot}H_2O$ (6.0 equiv), THF, H_2O, r.t., quant.

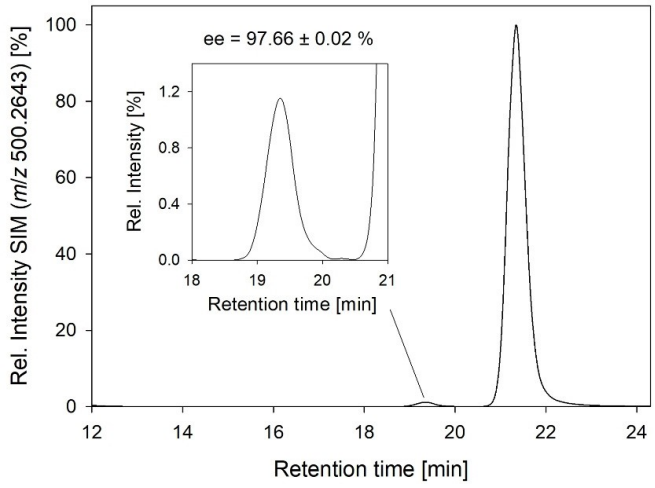

Figure 1. Separation of the thallusin enantiomers on a Chiralpak IA chiral amylose column under reversed phase conditions upon derivatization with iodomethane and determination of the enantiomer excess of the synthesis product. (−)-**1**, eluted at 21.23 min, was baseline separated from (+)-**1** for *ee* determination (insert).

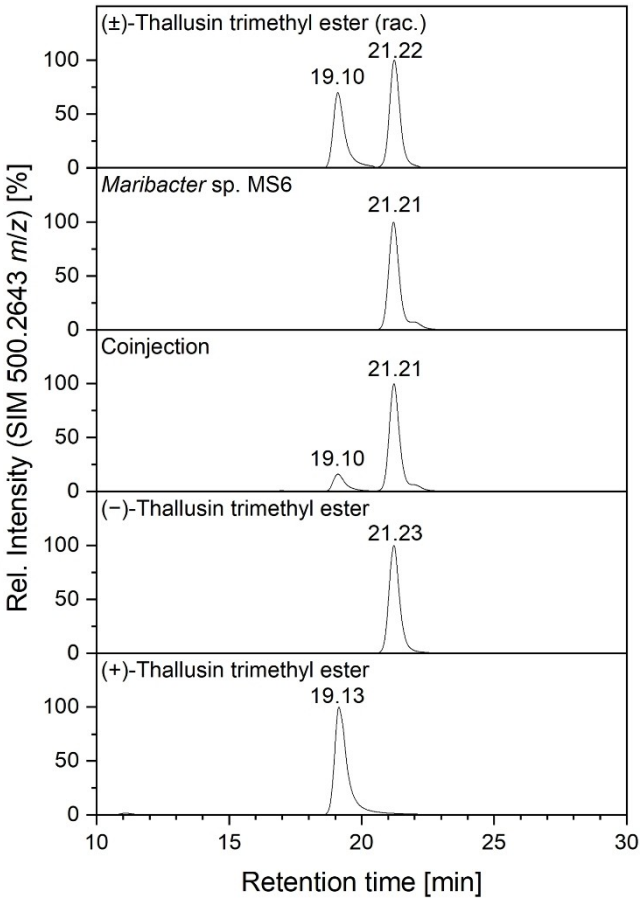

Figure 2. Stereoselective biosynthesis of thallusin. The trimethyl esters of thallusin were separated on a chiral amylose column and compared with reference standards. Thallusin was isolated from the bacterial supernatant and derivatized with iodomethane. Co-injection of the racemate with the bacterially produced thallusin revealed the stereoselective biosynthesis of (−)-thallusin by *Maribacter* sp. MS6, isolated from the microbiome of *Ulva mutabilis*.

synthetic (+)-**1**, as obtained before by us and by others,[16,17] could also retain traces of (−)-**1** that are analytically undetectable but eco-physiologically effective due to their enormous biological activity.[17]

We therefore scrutinized the analytical limit of detection (LOD) for (−)-thallusin (LOD = 0.18 nmol L^{-1} **(Table S1, Figure S1**) in the presence of an excess of (+)-thallusin (100 nmol L^{-1}, Table S1, Figure S1). The LOD was thus 36-fold higher than its biological activity (EC_{50} = 0.005 nmol L^{-1}). Additionally, due to (+)-thallusin peak tailing, the later eluting (−)-thallusin was only detected if the ratio of (−)-thallusin to (+)-thallusin was greater than 0.002. Hence, even at a very high chemical purity of (+)-thallusin, possibly remaining, biologically active traces of (−)-thallusin must be considered when (+)-thallusin is applied to bioactivity reasoning.

Enantiopurity of naturally occurring (−)-thallusin. Considering the enormous bioactivity of the (−)-isomer, biosynthesis would not need to be highly enantioselective. Different stereoisomers could even have different activities in different algae. However, a comparison of a bacterium-derived thallusin sample with the synthetic racemate demonstrated that *Maribacter* sp. MS6 secretes only the biologically active (−)-isomer (Figure 2). The same was true for other thallusin producers, such as *Zobellia galactanivorans* Dsij (data not shown). Notably, (+)-thallusin could not be detected by our methods in the supernatant, suggesting that the biosynthesis is indeed highly enantioselective (> 99.5 % *ee*).

Resorption of Fe-thallusin complexes. Previous studies have demonstrated that (−)-thallusin is biologically active in *Ulva*, whereas (+)-thallusin is not.[17] Furthermore, a narrow SAR was found. [17] We thus tested the bioactivity of nitrile **31**. Interestingly, the replacement of the carboxylic acid group with a nitrile group on the terpenoid backbone led to the complete loss of morphogenic activity, such as rhizoid or cell wall formation induction (Figure 3). Because this Fe(III)-complex of the derivative should be differently charged, we speculated that the steep loss of potency might be attributed to charge-specific cell transport or import. To gain deeper insights into the transport of (−)-thallusin in *Ulva* and SAR analysis, we performed dedicated short term uptake experiments in the presence of Fe(III) ions.

Previous research has indicated a 2:1 thallusin-Fe(III) complex formation, as well as its uptake from the phycosphere of *Ulva*.[7] Because the *in situ* concentration of thallusin is far lower than the background iron concentration in sea water, thallusin is largely present as an iron complex in *Ulva's* phycosphere. Consequently, short-term uptake experiments were performed using the stable isotope ^{58}Fe and ICP-MS analysis to determine how specific iron uptake is mediated by (−)-thallusin, (+)-thallusin, and by nitrile **31**. These experiments revealed that iron complexes of thallusin or of nitrile **31** are differently acquired by the gametes when compared to Fe-EDTA and ferric chloride (Figure 4). Interestingly, all derivatives that are able to form stable 2:1 Fe(III) complexes did strongly promote ^{58}Fe uptake. This result suggests that the algae

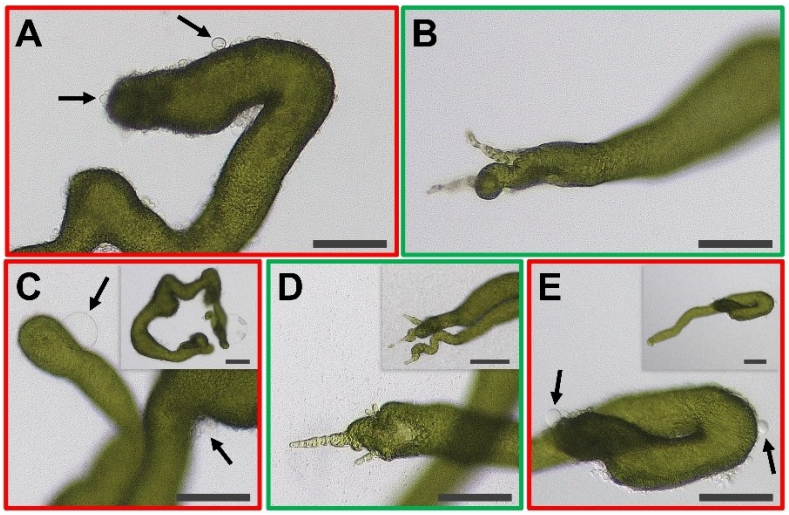

Figure 3. Morphogenetic bioassays with *Ulva compressa* (cultivar *mutabilis*). Axenic gametes were inoculated with (**A**) *Roseovarius* sp. MS2 only, (**B**) additional *Maribacter* sp. MS6 (tripartite community, OD_{620} (bacteria) = 0.0001), (**C**) (+)-thallusin, (**D**) (−)-thallusin or (**E**) its nitrile analogue **31** in replacement of *Maribacter* sp. MS6 (c = 0.010 nmol L^{-1} for all tested substances). Only (−)-thallusin induced rhizoid and cell wall formation (green framed). The absence of *Maribacter* sp. or (−)-thallusin resulted in cell wall protrusions (arrow, red framed). The inserts (**C**–**E**) show overview photographs of the respective induced morphotypes. Bars represent 100 μm.

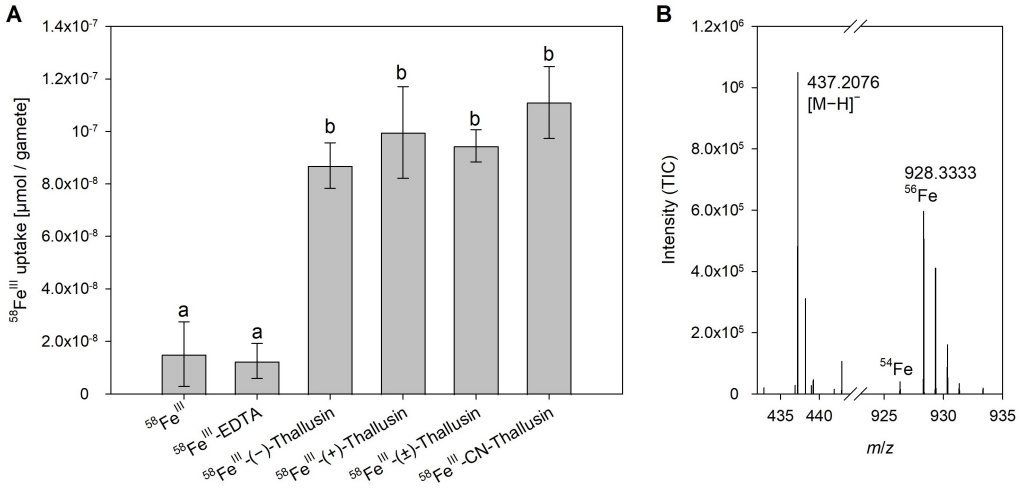

Figure 4. Short-term uptake experiments of iron complexes by gametes analyzed by ICP-MS. (**A**) *U. mutabilis* gametes acquired Fe–thallusin rapidly compared with iron hydroxide and Fe-EDTA during short-term uptake experiments (statistical test: one-way ANOVA with Tukey post-hoc test, error bars indicate the standard deviation; $n = 3$). Different letters show significant differences ($p < 0.05$). (**B**) Electrospray ionization mass of nitrile **31**, sampled from *Ulva* culture medium, detected in negative ionization mode as the free ligand (M) and as the 2 : 1 Fe complex $[Fe(\mathbf{31})_2\text{-}4H]^-$. Isotopologues containing ^{54}Fe or ^{56}Fe are indicated.

internalize all these thallusin derivatives as an Fe(III) complex, independent of stereochemistry or substitution (**31**).

Functional Implications. Environmental iron is made bioavailable by bacterial siderophores that form stable, soluble complexes. These complexes are used as a public good in microbial communities. Iron uptake genes coding for putative transporters have been found in the *Ulva* genome.[50] These data indicate that the macroalga can acquire iron provided by associated bacterial communities.[51] Our findings now suggest that the biological activity of thallusin is not controlled by cellular uptake, but results from intracellular processing of the signaling compound. Specific intracellular recognition of (−)-thallusin (or a coordination compound thereof) by a putative, ligand-dependent receptor is likely. The very high activity of thallusin and its morphogenetic activity might suggest nuclear receptors to be involved.[52]

Because of its very low (pM) concentration *in natura*, thallusin cannot play a significant role in iron homeostasis. However, the siderophore-mediated uptake may provide specific algal access to the externally supplied, very polar, and highly potent thallusin. Furthermore, the active import process may lead to an enrichment of thallusin in the algae cells itself, contributing to the very high activity observed. Additionally, our biological data strongly indicate that an iron complex can be internalized in *Ulva*, in addition to the reductive iron assimilation process.[50] Although the mechanistic details remain

to be clarified,[51] our results suggest that a rather non-selective siderophore uptake system might work as an active shuttle system for (−)-thallusin. These data indicate a non-selective primary cellular uptake of the metal complex preceeding a specific, secondary signal transduction process elicited only by (−)-thallusin inside the cell.

Conclusions

We developed a fully enantioselective, catalytic total synthesis that provides efficient access to (−)-thallusin. This development features a programmed precursor design for polyene cyclization, effective application of Carreira's Ir-complex mediated polyene cyclization on the gram scale, dedicated substrate transformation, and effective scaffold completion. This synthesis route can be used for molecular editing, as exemplified by the nitrile **31**, and is amenable to precursor variation. Notably, the final sp^2-sp^2 couplings necessitate a deconjugated vinyl electrophile to be productive.

By studying the compounds such obtained and by developing a reliable *ee* determination procedure, we found the bacterial biosynthesis of thallusin to be highly enantioselective. Notably, the uptake of iron mediated by thallusin derivatives was independent of their stereochemistry or substitution, whereas the morphogenic activity of thallusin was highly structure-dependent. These findings imply that thallusin is imported into algae cells as an iron complex, possibly via generally acting importers such as provided by siderophore transporters. It then unfolds its activity inside the algae after active enrichment in a more specific fashion. Further studies will reveal the processing of the signal and the receptors involved.

Experimental Section

Regio- and enantioselective polyene cyclization: $[Ir(COD)Cl]_2$ (39 mg, 0.06 mmol, 0.04 eq) and enantiopure ligand **11** (117 mg, 0.23 mmol, 0.16 eq) were stirred for 15 min in dichloroethane (8 mL). Allyl alcohol **5** (500 mg, 1.44 mmol, 1.0 eq) in dichloroethane (1 mL) and $Zn(OTf)_2$ (105 mg, 0.29 mmol, 0.20 eq) were added, and the mixture was stirred for 24 h at room temperature. TFA (220 μL, 2.88 mmol, 2.0 eq) was added, and stirring was continued for 2 h. The solvent was removed under reduced pressure and the residue was purified by flash column chromatography (petroleum ether: EtOAc = 99:1) to yield anisole **12** as a colorless oil (330 mg, 1.29 mmol, 89%, d.r. > 9:1).

Negishi coupling of deconjugated enol triflate: LiCl (52 mg, 1.22 mmol, 5.8 eq) was dried for 10 min at 150 °C under vacuum (0.1 mbar). Zinc powder (82 mg, 1.26 mmol, 6.0 eq) was added and the mixture was dried for further 10 min at 150 °C under vacuum. After cooling to room temperature and refilling the flask with N_2, degassed THF (5 mL), 1,2-dibromoethane (5 μL) and TMSCl (5 μL) were added. After vigorous stirring for 5 min, an iodine crystal was added and stirring was continued for 5 min. Dimethyl 3-bromopyridine-2,6-dicarboxylate (173 mg, 0.63 mmol, 3.0 eq) was added and the reaction mixture was stirred for 1 h at room temperature to give a dark red solution. Stirring was stopped and the supernatant was transferred to a solution of enol triflate **2** (90 mg, 0.21 mmol, 1.0 eq) and $Pd(PPh_3)_4$ (12 mg, 11 μmol, 5 mol%) in degassed THF (5 mL). The reaction mixture was stirred for 1 h at room temperature. Aqueous NH_4Cl solution (20 mL) was added and the aqueous layer was extracted with Et_2O (3×20 mL). The combined organic extracts were washed with aqueous 5% thiourea solution (30 mL), dried with Na_2SO_4, filtered, and concentrated under reduced pressure. The residue was purified by flash column chromatography (petroleum ether:EtOAc = 8:2) to give pyridine **30** as a yellow oil (74 mg, 0.16 mmol, 76%). as a mixture of epimers (ca. 3:2 by ^{1}H-NMR).

For further experimental details, including compound data, analytical and biological experimentation, see the Supporting Information.

Supporting Information

The authors have cited additional references within the Supporting Information.[7,24,35,41,49]

Acknowledgements

Doctoral fellowships from Deutsche Bundesstiftung Umwelt (to P.W.), from the Konrad-Adenauer-Stiftung (to J.F.U.), and from Chilean National Agency for Research and Development (ANID) and German Academic Exchange Service (DAAD)/Scholarship Program bilateral agreement between Becas Chile – DAAD 2017 (to C.F.M–R) are gratefully acknowledged. This work was supported by the European Commission (Marie-Curie fellowship grant no. 796194 THALLMORPHAL, to S.R.) and by the Deutsche Forschungsgemeinschaft (SFB 1127 ChemBioSys, to H.-D. A. and T.W., subprojects A01 and C03; EXC 2051 Balance of the Microverse, to H.-D. A.; equipment grant INST 275/442-1 FUGG). We would like to acknowledge the MS platform at Friedrich Schiller University Jena for support in mass spectrometry. The Q-Exactive GC mass spectrometer was funded by the state of Thuringia (2015 FGI 0021) with means of the EU in the framework of the EFRE program. Open Access funding enabled and organized by Projekt DEAL.

Conflict of Interests

The authors declare no conflict of interest.

Data Availability Statement

The data that support the findings of this study are available in the supplementary material of this article.

Keywords: algae · siderophores · polyene cyclization · terpenoids · total synthesis

[1] C. H. Greene, M. E. Huntley, I. Archibald, L. N. Gerber, D. L. Sills, J. Granados, J. W. Tester, C. M. Beal, M. J. Walsh, R. R. Bidigare, et al. *Oceanography* **2016**, *29*, 10–15.
[2] G. C. Dismukes, D. Carrieri, N. Bennette, G. M. Ananyev, M. C. Posewitz, *Curr. Opin. Biotechnol.* **2008**, *19*, 235–240.
[3] B. J. Walsh, F. Rydzak, A. Palazzo, F. Kraxner, M. Herrero, P. M. Schenk, P. Ciais, I. A. Janssens, J. Peñuelas, A. Niederl-Schmidinger, M. Obersteiner, *Carbon Balance Manage.* **2015**, *10*, 26.
[4] B. Charrier, M. H. Abreu, R. Araujo, A. Bruhn, J. C. Coates, O. De Clerck, C. Katsaros, R. R. Robaina, T. Wichard, *New Phytol.* **2017**, *216*, 967–975.
[5] F. Ghaderiardakani, G. Califano, J. F. Mohr, M. H. Abreu, J. C. Coates, T. Wichard, *Aquac. Environ. Interact.* **2019**, *11*, 375–391.
[6] V. Smetacek, A. Zingone, *Nature* **2013**, *504*, 84–88.
[7] T. Alsufyani, G. Califano, M. Deicke, J. Grueneberg, A. Weiss, A. H. Engelen, M. Kwantes, J. F. Mohr, J. F. Ulrich, T. Wichard, *J. Exp. Bot.* **2020**, *71*, 3340–3349.
[8] Y. Kinoshita, Y. Sato, T. Sakurai, T. Yamasaki, H. Yamamoto, M. Hiraoka, *Cytologia* **2022**, *87*, 17–22.
[9] Y. Matsuo, H. Imagawa, M. Nishizawa, Y. Shizuri, *Science* **2005**, *307*, 1598.
[10] T. Wichard, *Semin. Cell Dev. Biol.* **2023**, *134*, 69–78.
[11] A. Weiss, R. Costa, T. Wichard, *Bot. Mar.* **2017**, *60*, 197–206.
[12] T. Wichard, *Front. Plant Sci.* **2015**, *6*, 86.
[13] X. Gao, Y. Matsuo, B. B. Snider, *Org. Lett.* **2006**, *8*, 2123–2126.
[14] X. Gao, Y. Matsuo, B. B. Snider, *Org. Lett.* **2007**, *9*, 379.
[15] M. Nishizawa, T. Iyenaga, T. Kurisaki, H. Yamamoto, M. Sharfuddin, K. Namba, H. Imagawa, Y. Shizuri, Y. Matsuo, *Tetrahedron Lett.* **2007**, *48*, 4229–4233.
[16] H. Yamamoto, Y. Takagi, T. Oshiro, T. Mitsuyama, I. Sasaki, N. Yamasaki, A. Yamada, H. Kenmoku, Y. Matsuo, Y. Kasai, H. Imagawa, *J. Org. Chem.* **2014**, *79*, 8850–8855.
[17] S. Dhiman, J. F. Ulrich, P. Wienecke, T. Wichard, H.-D. Arndt, *Angew. Chem. Int. Ed.* **2022**, *61*, e202206746.
[18] P. Wienecke, H. Görls, H.-D. Arndt, *Bioorg. Med. Chem. Lett.* **2022**, *72*, 128845.
[19] W. S. Johnson, *Bioorg. Chem.* **1976**, *5*, 51–98.
[20] C. N. Ungarean, E. Southgate, D. Sarlah, *Org. Biomol. Chem.* **2016**, *14*, 5454–5467.
[21] G. Gamboni, H. Schinz, A. Eschenmoser, *Helv. Chim. Acta.* **1954**, *37*, 964–971.
[22] P. A. Stadler, A. Eschenmoser, H. Schinz, G. Stork, *Helv. Chim. Acta.* **1957**, *40*, 2191–2198.
[23] R. A. Yoder, J. N. Johnston, *Chem. Rev.* **2005**, *105*, 4730–4756.
[24] M. A. Schafroth, D. Sarlah, S. Krautwald, E. M. Carreira, *J. Am. Chem. Soc.* **2012**, *134*, 20276–20278.
[25] R. J. Mills, N. Taylor, V. Snieckus, *J. Org. Chem.* **1989**, *54*, 4372–4385.
[26] M. S. Loft, T. J. Mowlem, D. A. Widdowson, *J. Chem. Soc. Perkin Trans. 1* **1995**, 97–104.
[27] E. Bures, J. A. Nieman, S. Yu, P. G. Spinazzé, J.-L. J. Bontront, I. R. Hunt, A. Rauk, B. A. Keay, *J. Org. Chem.* **1997**, *62*, 8750–8759.
[28] H. Ishibashi, H. Sakashita, M. Ikeda, *J. Chem. Soc. Perkin Trans. 1* **1992**, 1953–1957.
[29] M. Herrlich, N. Hampel, H. Mayr, *Org. Lett.* **2001**, *3*, 1629–1632.
[30] S. P. Fearnley, M. W. Tidwell, *Org. Lett.* **2002**, *4*, 3797–3798.
[31] J. B. Lambert, *Tetrahedron* **1990**, *46*, 2677–2689.
[32] M. Uemura, S. Tokuyana, T. Sakan, *Chem. Lett.* **1975**, *4*, 1195–1198.
[33] J.-E. Bäckvall, M. Sellén, B. Grant, *J. Am. Chem. Soc.* **1990**, *12*, 6615–6621.
[34] Y. Lai, N. Zhang, Y. Zhang, J.-H. Chen, Z. Yang, *Org. Lett.* **2018**, *20*, 4298–4301.
[35] A. Abad, C. Agulló, M. Arnó, A. C. Cuñat, R. J. Zaragozà, *J. Org. Chem.* **1989**, *54*, 5123–5125.
[36] C. W. J. Chang, S. W. Pelletier, *Tetrahedron Lett.* **1966**, *7*, 5483–5487.
[37] T. Ueda, H. Konishi, K. Manabe, *Org. Lett.* **2012**, *14*, 5370–5373.
[38] S. Dharuman, Y. D. Vankar, *Org. Lett.* **2014**, *16*, 1172–1175.
[39] D. L. J. Clive, Minaruzzaman, H. Yang, *J. Org. Chem.* **2008**, *73*, 6743–6752.
[40] H. M. R. Hoffmann, K. Giesel, R. Lies, Z. M. Ismail, *Synthesis* **1986**, 548–551.
[41] P. Wienecke, H.-D. Arndt, *Org. Lett.* **2023**, *25*, 1188–1191.
[42] A. Krasovskiy, P. Knochel, *Angew. Chem. Int. Ed.* **2004**, *43*, 3333–3336.
[43] J. Takagi, K. Takahashi, T. Ishiyama, N. Miyaura, *J. Am. Chem. Soc.* **2002**, *124*, 8001–8006.
[44] F. W. Lichtenthaler, M. Lergenmüller, S. Schwidetzky, *Eur. J. Org. Chem.* **2003**, 3094–3103.
[45] O. M. Berner, L. Tedeschi, D. Enders, *Eur. J. Org. Chem.* **2002**, 1877–1894.
[46] J. C. Anderson, A. J. Blake, M. Mills, P. D. Ratcliffe, *Org. Lett.* **2008**, *10*, 4141–4143.
[47] J. M. Aizpurua, M. Oiarbide, C. Palomo, *Tetrahedron Lett.* **1987**, *28*, 5361–5364.
[48] F. A. Davis, M. Serajul Haque, T. G. Ulatowski, J. C. Towson, *J. Org. Chem.* **1986**, *51*, 2402–2404.
[49] J. F. Ulrich, M. S. Gräfe, S. Dhiman, P. Wienecke, H.-D. Arndt, T. Wichard, *Mar. Drugs* **2022**, *20*, 690.
[50] O. De Clerck, S. M. Kao, K. A. Bogaert, J. Blomme, F. Foflonker, M. Kwantes, E. Vancaester, L. Vanderstraeten, E. Aydogdu, J. Boesger, G. Califano, B. Charrier, R. Clewes, A. del Cortona, S. D'Hondt, N. Fernandez-Pozo, C. M. Gachon, M. Hanikenne, L. Lattermann, F. Leliaert, X. Liu, C. A. Maggs, Z. A. Popper, J. A. Raven, M. van Bel, P. K. I. Wilhelmsson, D. Bhattacharya, J. C. Coates, S. A. Rensing, D. van der Straeten, A. Vardi, L. Sterck, K. Vandepoele, Y. van de Peer, T. Wichard, J. H. Bothwell, *Curr. Biol.* **2018**, *28*, 2921–2933.
[51] T. Wichard, *Front. Mar. Sci.* **2016**, *3*, 131.
[52] C. Glass, M. Rosenfeld, *Genes Dev.* **2000**, *14*, 121–141.

Manuscript received: December 21, 2023
Accepted manuscript online: January 25, 2024
Version of record online: February 13, 2024